magnetochemistry

MDPI

Review

Magnetic Switchability via Thermal-Induced Structural Phase Transitions in Molecular Solids

Shan-Nan Du, Chan-Ying Yao, Jun-Liang Liu * and Ming-Liang Tong

Key Laboratory of Bioinorganic and Synthetic Chemistry of Ministry of Education, School of Chemistry, Sun Yat-Sen University, Guangzhou 510006, China

* Correspondence: liujliang5@mail.sysu.edu.cn

Abstract: Magnetically switchable molecular solids with stimuli-responsive ON/OFF characteristics are promising candidates for smart switches and magnetic storage. In addition to conventional spin-crossover/charge-transfer materials whose magnetic responses arise from changes in the electronic structure of the metal centers, peripheral chemical entities that exhibit tunability provide an alternative and promising tactic for the construction of magnetic multi-stable materials. Temperature changes can trigger a reversible structural phase transition that can affect the coordination environment of a transition-metal center because of the thermal-induced motion of ligands, counterions, neutral guests, and/or changes in coordination number, thus potentially realizing magnetic bistability which can arise from a concomitant spin state change or the modulation of orbital angular momentum. Perspectives and challenges are also highlighted to provide insights into its development.

Keywords: structural phase transition; switchable magnetic molecule; spin-orbital coupling; spin state; thermal-induced motion

check for updates

Citation: Du, S.-N.; Yao, C.-Y.; Liu, J.-L.; Tong, M.-L. Magnetic Switchability via Thermal-Induced Structural Phase Transitions in Molecular Solids. *Magnetochemistry* **2023**, *9*, 80. https://doi.org/10.3390/magnetochemistry9030080

Academic Editor: Andrea Caneschi

Received: 9 February 2023
Revised: 2 March 2023
Accepted: 7 March 2023
Published: 9 March 2023

1. Introduction

Switchable molecular solids with significant magnetic switchability exhibit rich and controllable stimuli-responsive behaviors under external perturbations such as heat [1–3], light [4–6], or pressure [7–9]. This field can realize the modulation and manipulation of molecular structures, electron energy levels and macroscopic magnetoelectric properties and has broad application prospects in sensors, magneto-memory materials, molecular switches, and spintronic devices [2–4]. Molecular magnets sandwiched between two metallic electrodes via covalent bonding or two ferromagnetic electrodes have been realized in recent years [10,11]. Molecular spintronic devices have emerged as having a high potential for electronic control of molecular magnets associated with different spin states. For a more in-depth study, the dynamic changes in the magneto-structural relationship and other relevant physical properties of many multi-stable complexes have been reported in detail.

The magnetic switchability of many coordination complexes is closely associated with the reversible regulation of electronic structures, crystal field (CF), orbital angular momentum and magnetic anisotropy. The best-known system is the conventional spin-crossover (SCO) complex. When the 3d transition metal centers with d^4-d^7 electronic configuration have an appropriate ligand field strength, a similar splitting energy and spin pairing energy can enable a spin multiplicity switch between high-spin (HS) and low-spin (LS) states under external stimulation, producing a significant magnetic response (Figure 1b) [1–3]. Another representative example is the charge transfer (CT) complex, which exhibits redox state transitions in response to external stimuli [9,12–15]. Although the magnetic switching of most conventional SCO and CT materials can also be accompanied by structural changes, these magnetic switchable properties are driven by the electron rearrangement of the metal centers induced by external stimuli, and thus the choices of metal centers and ligands are limited.

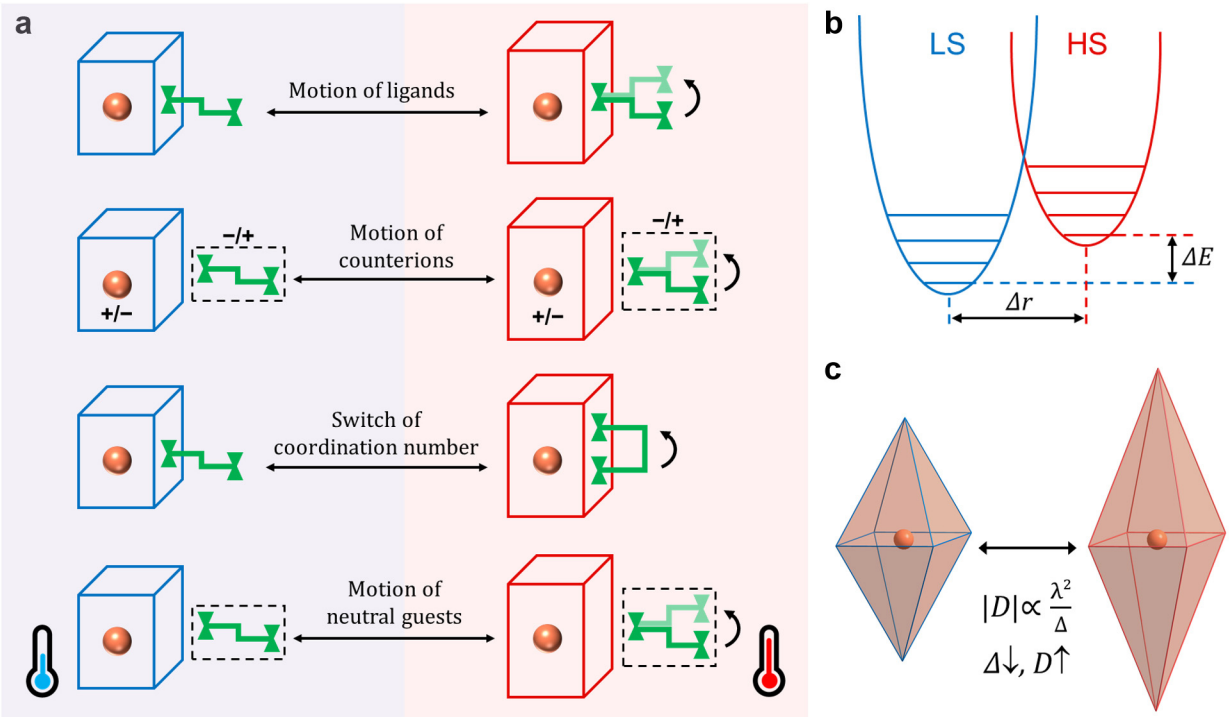

Figure 1. (**a**) Schematic representation of four types of thermal-induced dynamics of ligands, counterions, coordination number and neutral guests in switchable magnetic molecules. Orange atoms represent the metal centers. The blue and red boxes represent the coordination environment of the metal center at the low-temperature and high-temperature phases, respectively, which can be reversibly switched with the thermal-induced structural phase transition. (**b**) Energy potential well of spin crossover complexes for high-spin (HS) and low-spin (LS) states ($d^{4\sim7}$) with lattice vibration. (**c**) Schematic illustration of changes in the coordination environment of 3d metal centers accompanied by changes in spin–orbit coupling and magnetic anisotropy.

Apart from the two typical magnetic multi-stable materials dominated by electronic structure changes, the inherent structural changes of tunable molecules can also be used to induce spin transition and the modulation of orbital angular momentum to achieve magnetic switchability (Figure 1) [14–16]. On the one hand, the inherent structural change in the molecule does not depend on the rearrangement of the electronic structure of the metal center, which greatly improves the design diversity of switchable magnetic molecules. On the other hand, its combination with spin state transition or the modulation of orbital angular momentum provides a rich and efficient approach to realize switchable magnetic materials.

From the thermodynamic point of view, the first-order phase transition occurs when the first derivative of thermodynamic potential, such as entropy or volume, is discontinuous at the critical temperature (T_c); the second-order phase transition happens if the first derivative is continuous while there is a singular point in the second derivative, such as specific heat [17,18]. The Landau theory proposed the concept of an "order parameter" to describe phase transition [19,20], in which the thermodynamic potential is a function of the order parameter. In the high-temperature phase (the order parameter is zero), the substance exhibits a low degree of order and high symmetry. In the low-temperature phase, the degree of order increases (the order parameter is non-zero), which leads to the occurrence of symmetry breaking. In a crystal, structural phase transition refers to the transformation of crystal structure between different phases in response to external perturbations, accompanied by changes in physical properties without any changes in chemical compositions [21,22].

How is the orbital angular momentum of coordination complexes modulated upon phase transition? Both the electron spin magnetic moment and the orbital magnetic moment contribute to the magnetism of matter. However, the crystal field can act on the central metal orbitals, leading to the removal of its degeneracy, the partial quenching of orbital magnetic moment and the rearrangement of energy levels [23–27]. The cooperation of spin–orbit coupling (SOC) and crystal-field (CF) effect results in zero-field splitting (ZFS). For most 3d ions, the latter is much stronger than the former [23–25]. For example, when the distorted octahedral 3d ion is further elongated, the energy gap (Δ) between the excited and the ground terms caused by crystal-field splitting decreases (Figure 1c). Since the ZFS parameter D is inversely proportional to Δ, D increases and the magnetic anisotropy enhances accordingly.

$$\widehat{H}_{ZFS} = D\left[\hat{S}_z^2 - \frac{1}{3}S(S+1)\right] + E\left(\hat{S}_x^2 - \hat{S}_y^2\right) \quad (1)$$

The change in the coordination environment is often accompanied by the modulation of the crystal field, which may directly or indirectly affect the contribution of orbital angular momentum and the change in magnetic anisotropy [12–16,28–30]. Therefore, modulating orbital angular momentum by affecting the coordination geometry of the metal center through structural phase transition is an effective strategy for constructing switchable magnetic molecules.

Inspired by the intriguing working mechanisms and fascinating functions of biological molecular machines, various artificial molecular machines (AMMs) with switchable properties have developed over the last few decades [31–37]. One of the visions in this field is to amplify microscopic molecular-scale motion to controllable modulation of macroscopic physical properties under appropriate external stimuli, thus promoting its potential application in smart materials and responsive molecular systems. This idea of precisely controlling the ON/OFF behavior coincides with the design strategy of switchable magnetic materials. By introducing AMMs into magnetic complexes, there may be a great opportunity to trigger structural phase transitions, leading to controllable and reversible magnetism dynamics and diverse functionalities.

For most molecular solids, the control over magnetism is triggered by heat. However, the optical, pressure, electrical, and magnetic control of molecular magnetic properties are also fascinating topics. For instance, a lot of efforts have been devoted to studying light-induced excited spin-state trapping (LIESST) effect, light-induced valence tautomerism, pressure-induced spin transition and magnetic-field-induced valence tautomerism, etc. [7]. Since thermal stimulation is more widely used, we focus on typical types of thermal-induced structural phase transition (first-order phase transition) in this review. These phase transition behaviors affect the coordination environment of metal centers and lead to the spin state transition or the modulation of orbital angular momentum. It is noted that although the examples of solvation/desolvation, etc., show single-crystal-to-single-crystal (SCSC) structural transformations, they would not be described herein due to the changes in chemical compositions [38–40]. Depending on what triggers the structural phase transition, we outline four thermal-induced dynamics of ligands, counterions, coordination numbers and neutral guests, respectively (Figure 1). Finally, our perspectives and suggestions for the further developments of this family are put forward.

2. Thermal-Induced Dynamics of Ligands

The flexibility of intramolecular building blocks is crucial to the stimulus-responsive behavior of molecular structures [41,42]. The resulting changes in the molecular structure and the packing mode can directly or indirectly affect the coordination geometry of the metal centers and the synergistic effect, thus generating the regulation of various physical properties [43]. Numerous complexes that undergo such dynamic structural changes in ligands have been reported.

Depending on the species of thermal-induced-motion ligands, this section is divided into two categories: the alkyl chains and the non-alkyl groups.

2.1. Alkyl Chains

The rotation around C-C bonds is considered to be one of the most studied molecular motions [44]. Since the alkyl chains are unstable and prone to multi-conformational changes in the ground electronic state, entropy can be stored to adjust the relative thermodynamic stability of the aggregate state of the complexes [45]. Moreover, the coordination environment of the metal centers with long alkyl chains may show synchronization with the alkyl chains. These backgrounds provide an excellent platform for investigating magnetic multi-stable alkylated complexes. Some dynamic complexes based on alkyl chains have been described due to their lability as well as their potential for multiple conformational changes.

The long alkyl chain ligand complex $[Co(C_{16}\text{-terpy})_2](BF_4)_2$ (C_{16}-terpy = 4′-hexadecyloxy-2,2′:6′,2″-terpyridine) was first reported by Hayami and coworkers in 2005 [43]. Notably, the reverse spin transition (rST) ($T_{\downarrow}$ = 217 K, $T_{\uparrow}$ = 260 K, ΔT = 43 K) was observed for the first time in this complex, which is by virtue of the structural phase transition related to the entropy-driven motion of the alkyl chains (Figure 2a). In addition, the complex $[Co(C_{14}\text{-terpy})_2](BF_4)_2$ also exhibits similar rST behavior with a wider hysteresis ($T_{\downarrow}$ = 250 K, $T_{\uparrow}$ = 307 K, ΔT = 57 K).

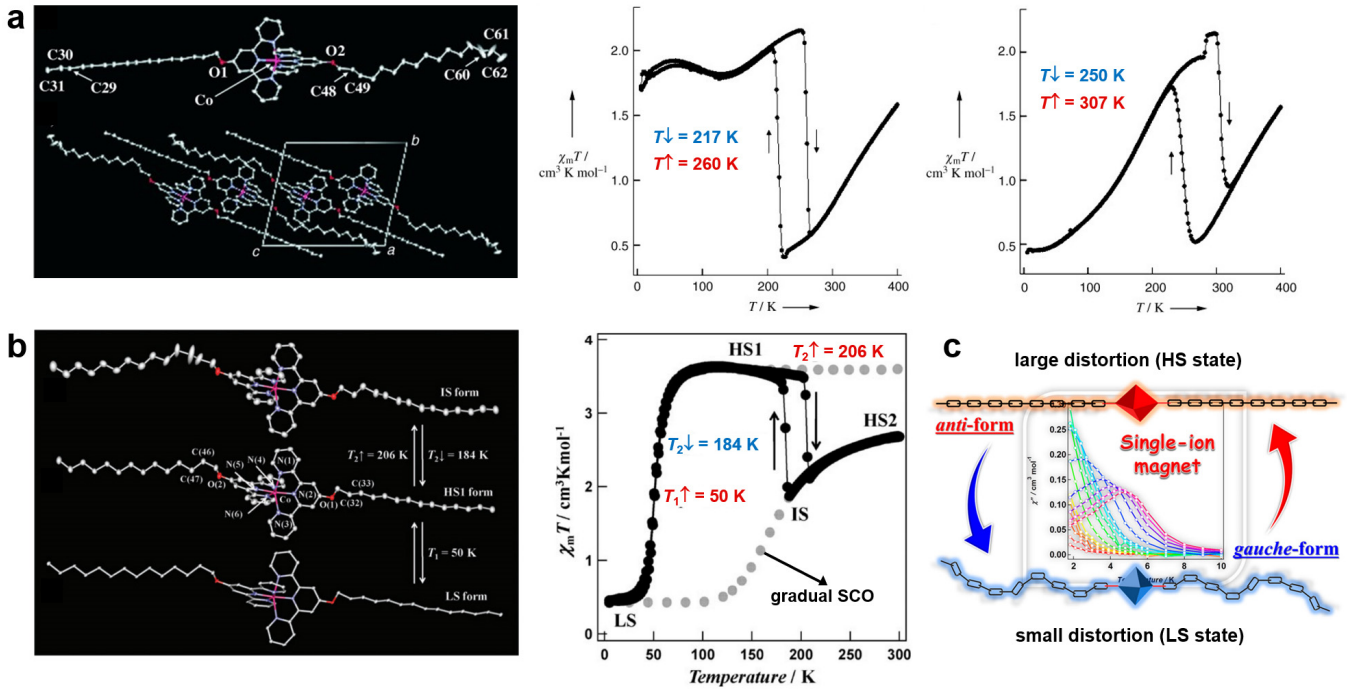

Figure 2. (**a**) **Left**: molecular structure of $[Co(C_{16}\text{-terpy})_2](BF_4)_2{\cdot}MeOH$ and its packing in the crystal. **Middle and Right**: the reverse spin transition (rST) properties of $[Co(C_{16}\text{-terpy})_2](BF_4)_2$ and $[Co(C_{14}\text{-terpy})_2](BF_4)_2$, respectively. Reproduced with permission from [43]. (**b**) **Left**: molecular structures of $[Co(C_{14}\text{-terpy})_2](BF_4)_2{\cdot}MeOH$ in low−spin (LS), high−spin (HS) and incomplete spin (IS) states, respectively. **Right**: the SCO behavior and incomplete rST behavior. Reproduced with permission from [46]. (**c**) Schematic representation of the rST initiated by the structural transition of the alkyl chain conformations and the field−induced slow magnetic relaxation of $[Co(C_{16}\text{-terpy})_2](BF_4)_2$. Reproduced with permission from [47].

Three years later, they reported a similar long alkyl chain Co^{II} complex $[Co(C_{14}\text{-terpy})_2](BF_4)_2{\cdot}MeOH$ (C_{14}-terpy = 4′-tetradecyloxy-2,2′:6′,2″-terpyridine) with two high-spin states (HS_1 and HS_2) [46]. HS_1 and HS_2 states exhibit abrupt ($T_{1\uparrow}$ = 50 K) and gradual ($T_{\uparrow}$ = 175 K) SCO behavior, respectively (Figure 2b). The SCO behavior at $T_{1\uparrow}$ = 50 K

(without hysteresis) is only due to the shortening of the Co-N bond lengths caused by the change in the interaction between the alkyl chains. The incomplete rST with thermal hysteresis of 22 K between $T_{2\uparrow}$ = 206 K and $T_{2\downarrow}$ = 184 K owes to the structural phase transition induced by the thermal motion of alkyl chains. In the IS (incomplete spin) phase, the symmetry of the coordination environment around the Co^{II} ion is higher.

Interestingly, based on previous studies, an unprecedented work of field-induced slow magnetic relaxation coexisting with rST was reported in 2019 (Figure 2c) [47]. After changing from the high-temperature phase (LS state) to the low-temperature phase (HS state), the packing mode of the alkyl chains in $[Co(C_{16}\text{-terpy})_2](BF_4)_2$ changed from *gauche*-form to *anti*-form. The structural phase transition triggered the large distortion of the coordination geometry of Co^{II} ions and the rST behavior. The resulting enhancement of magnetic anisotropy makes the complex exhibit typical field-induced single-ion magnet (SIM) behavior. Collectively, these works all induce interesting magnetic properties through the movement of the long alkyl chains, which confirm the feasibility of introducing flexible alkyl ligands into complexes.

In 2013, Real et al. synthesized an alkylated complex $[Fe(n\text{Bu-im})_3(tren)](PF_6)_2$ (*n*Bu-im = *n*-buthylated 1*H*-imidazol-2-aldehyde, tren = tris(2-ethylamino)amine) [48]. By simply altering the sweep rate of temperature, two independent and strong cooperative SCO behaviors can be separated (Figure 3b). One of them is between the HS state and the LS_1 state with a hysteresis of 14 K ($T_{\downarrow}$ = 115 K and $T_{\uparrow}$ = 129 K) at the sweep rate of 4 $K{\cdot}min^{-1}$, while the other is between the same HS state and the different LS_2 state with a wider hysteresis (ΔT = 41 K, $T_{\downarrow}$ = 135 K and $T_{\uparrow}$ = 176 K) at 0.1 $K{\cdot}min^{-1}$. In addition, at the intermediate sweep rates, the two hysteresis loops will be partially merged. Such unique magnetic properties could be attributed to the conformational changes in alkyl chains and the reorganization of the intermolecular interactions (Figure 3a). Although the SCO behaviors of this complex occur at temperatures far below room temperature, which limits its further practical application, this work presents a new system with magnetic multi-stability.

In 2018, magnetic tristability was achieved at room temperature by utilizing SCO behavior and ligand-driven magnetic changes for the first time (Figure 3d). Clérac and coworkers designed an iron(II) complex $[Fe(C_{10}\text{-pbh})_2]$ (C_{10}-pbh = (1*Z*,*N*′*E*)-4-(decyloxy)-*N*′-(pyridin-2-ylmethylene)-benzo-hydrazonate) with one LS phase and two HS-LS phases (denoted, respectively, as HS-LS_1 phase and HS-LS_2 phase) [49]. Upon cooling to 290 K, due to the entropy-driven isomerization of the decyloxy chains from a *gag* conformation to a more stable *aaa* conformation, the complex changes from HS-LS_1 phase ($P2_12_12$) to HS-LS_2 phase ($P2_1$) (Figure 3c). The symmetry breaking affects the intermolecular interactions (including C-H···Fe and C-H···O) and results in the modification of the coordination sphere of Fe^{II}, thereby realizing non-SCO magnetic bistability (Figure 3d). With continued cooling to 220 K, the "breathing" of the alkyl chains leads to the deformation of the crystal packing, which is accompanied by the second symmetry breaking and the appearance of the LS phase ($P2_1/n$). Both Fe-N bond lengths and the large distortion of the coordination environment suggest a typical SCO behavior. However, only the SCO behavior of LS→HS-LS_1 ($P2_1/n \rightarrow P2_12_12$) was observed upon heating. This complex has a wide thermal hysteresis (ca. 35 K) around room temperature, which is rare in molecular magnetic materials.

Similarly, a mononuclear iron(II) complex with one-step incomplete SCO behavior, $[Fe^{II}(H_2Bpz_2)_2(C_9bpy)]$ (H_2Bpz_2 = dihydrobis(1-pyrazolyl) borate, C_9bpy = 4,4′-dinonyl-2,2′-bipyridine), was reported by Yao and Tao et al. in 2021 [50]. The slow dynamics in magnetic switchability can be attributed to the entropy-driven isomerization of long alkyl chains. Magnetic measurements show that various approaches, such as varying the scan rate, can accelerate the spin equilibrium of this complex, thus effectively improving the SCO completeness.

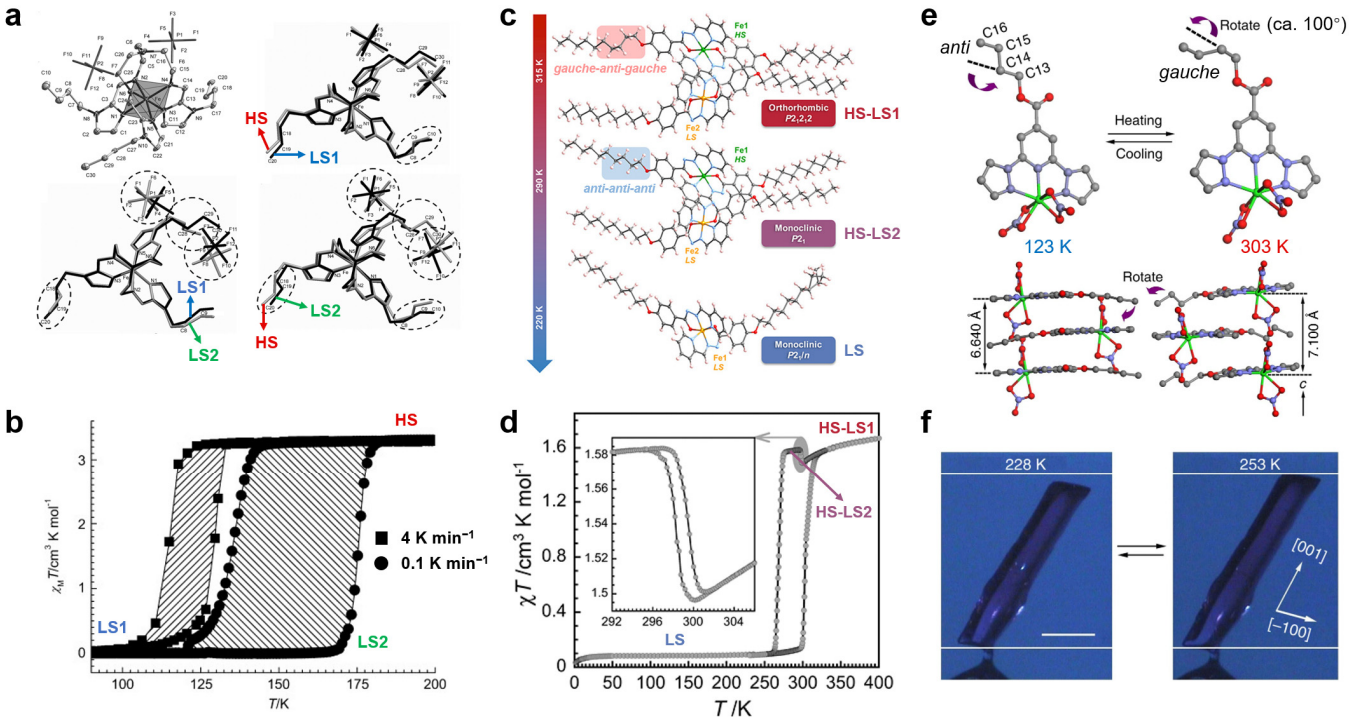

Figure 3. (**a**) Overlapping diagrams of [Fe(*n*Bu-im)$_3$(tren)](PF$_6$)$_2$ between different spin states (including LS$_1$, LS$_2$ and HS states) and (**b**) the SCO behaviors under different sweep rates. (**c**) Dynamic changes in the molecular structures of [Fe(C$_{10}$-pbh)$_2$] on decreasing temperature and (**d**) the magnetic multistability near room temperature. (**e**) The molecular structures and the packing diagrams along the crystallographic *c*−axis of [Co(NO$_3$)$_2$(*n*-butyl-2,6-di(1*H*-pyrazol-1-yl)isonicotinate)] in the low− and high−temperature phases and (**f**) the length of single crystal along the crystallographic [001] direction undergoes reversible expansion and contraction. (**a**,**b**) Reproduced with permission from [48]. (**c**,**d**) Reproduced with permission from [49]. (**e**,**f**) Reproduced with permission from [51].

Other than the research into the above alkylated SCO complexes, an interesting work on converting the alkyl rotation to a non-SCO behavior was published by Sato et al. They used the potential of alkyl chains as rotors to design an *n*-butyl functionalized divalent cobalt complex [Co(NO$_3$)$_2$(*n*-butyl-2,6-di(1*H*-pyrazol-1-yl)isonicotinate)] [51]. By heating from 123 K to 303 K, the *n*-butyl group rotates approximately 100° around the C13–C14 bond and its conformation changes from the ordered *anti*-form to the disordered *gauche*-form (Figure 3e). To reduce intermolecular repulsion to accommodate the rotation of the *n*-butyl group occupying more space, the adjacent intermolecular distance along the crystallographic *c*-axis increases. This extends to the positive thermal expansion of the crystal size along the *c*-axis (6~7%) through cooperative intermolecular interactions (Figure 3f). In addition, the crystal size expands by 5% along the *a*-axis. The change in the coordination environment of the metal center leads to the modulation of the orbital angular momentum near the phase transition point.

The structural flexibility of alkyl chains is an important factor affecting the coordination environment and intramolecular/intermolecular interactions of the complexes. Furthermore, on heating, the entropy increase originating from its conformational change can partially supplement the enthalpy increase in the first-order phase transition. It is feasible to use long alkyl chains to modify ligands to fabricate novel and intriguing functional materials. On the one hand, it provides the possibility for conformational isomerization or altering the molecular packing, which will affect the SCO centers, and then generates reversible thermo-responsive SCO behaviors through the intermolecular cooperative effect [48]. On the other hand, the use of alkyl chains may modulate the orbital angular

momentum by altering the coordination environment of the metal center, thus enabling the response of magnetic properties to thermal stimuli [51].

2.2. Non-Alkyl Groups

In addition to alkyl chains, incorporating other types of temperature-sensitive rotatable portions into the ligands also has the potential to trigger structural phase transitions, which demonstrates the universality of this method. More crucially, the utilization of non-alkyl group functionalized ligands can result in greater structural diversity in the complexes.

Most of the reported spin crossover complexes have small hysteresis width and are not in the vicinity of room temperature, which hinders their application. Recently, Real et al. realized a record-wide thermal hysteresis of 105 K spanning the room temperature range by introducing a built-in switching mechanism in the spin transition system to lock/unlock the deformation between LS state (less distorted) and HS state (strongly trigonally distorted) (Figure 4a) [52]. When the solvent-free iron(II) neutral complex [Fe^{II}(2-(5-(3-methoxy-4*H*-1,2,4-triazol-3-yl)-6-(1*H*-pyrazol-1-yl))pyridine)] is heated above 550 K, an exothermic monotropic transformation is observed, accompanied by the decrease in crystallographic symmetry from orthorhombic *Pbcn* to monoclinic $P2_1/c$. This complex exhibits an outstandingly wide and reproducible thermal hysteresis of 105 K ($T_{\downarrow}$ = 255 K, $T_{\uparrow}$ = 360 K). Structural analysis suggests that the hexagonal arrangement of the supramolecular chains leads to the steric coupling of the conformational change and the peripheral 3-methoxy groups (3MeO). When the 3MeO groups are in the elongated conformation, they lock the strongly trigonally distorted Fe^{II} from the adjacent molecules and maintain the HS state in a wide temperature range (Figure 4a). Upon choosing the bent conformation, the adjacent molecules have enough space to return to a less distorted geometry and switch to the LS state, namely, the large trigonal distortion of the central ions is unlocked. The most impressive aspect of this work is the purposeful programming of the thermal bistability of spin transition by employing the supramolecular latch mechanism, which offers a prospect for constructing new systems with practical applicability.

Recently, some attempts to create multi-stable molecular materials by introducing order–disorder type structural phase transition in combination with spin crossover have been reported. One of the interesting works is the mixed-valence trinuclear iron complex {$Fe^{III}_2Fe^{II}$} designed by Zhang et al. in 2022 (Figure 4b) [53]. According to the single crystal X-ray diffraction data, the solvent-free complex {[(pzTp)$Fe^{III}(CN)_3$]$_2$[Fe^{II}(L)]} ($pzTp^-$ = tetrapyrazoylborate, L = *N*,*N*′-bis-benzyl-*N*,*N*′-bis(2-picolyl)-ethylene-diamine) was obtained by heating {[(pzTp)$Fe^{III}(CN)_3$]$_2$[Fe^{II}(L)]}·2CH_3OH·5H_2O to 350 K. An irreversible desolvation-involved SCO transition from $LS_1{}^0$ phase ({$Fe^{III}_{LS}Fe^{II}_{LS}Fe^{III}_{LS}$}) to HS_1 phase ({$Fe^{III}_{LS}Fe^{II}_{HS}Fe^{III}_{LS}$}) occurred in this process, which was accompanied by the disorder of pyrazolyl rings in pzTp ligands. Magnetic measurements show that there is a reversible three-step transition with wide thermal hysteresis in the solvent-free complex {$Fe^{III}_2Fe^{II}$} (Figure 4b), which is attributed to one structural phase transition and a two-step SCO process. Interestingly, the wide thermal hysteresis associated with the former is near room temperature ($T_{\downarrow}$ = 256 K, $T_{\uparrow}$ = 300 K, ΔT = 44 K), and its width shows a hidden switchable behavior depending on the scanning rate. The unique SCO behaviors all occur due to the reconstruction and the adjustment of the supramolecular framework, which is closely related to the intermolecular contacts and $\pi\cdots\pi$ stacking of aromatic rings. This study successfully assembles magnetic multi-stable molecules via a dual mechanism based on spin and non-spin transitions.

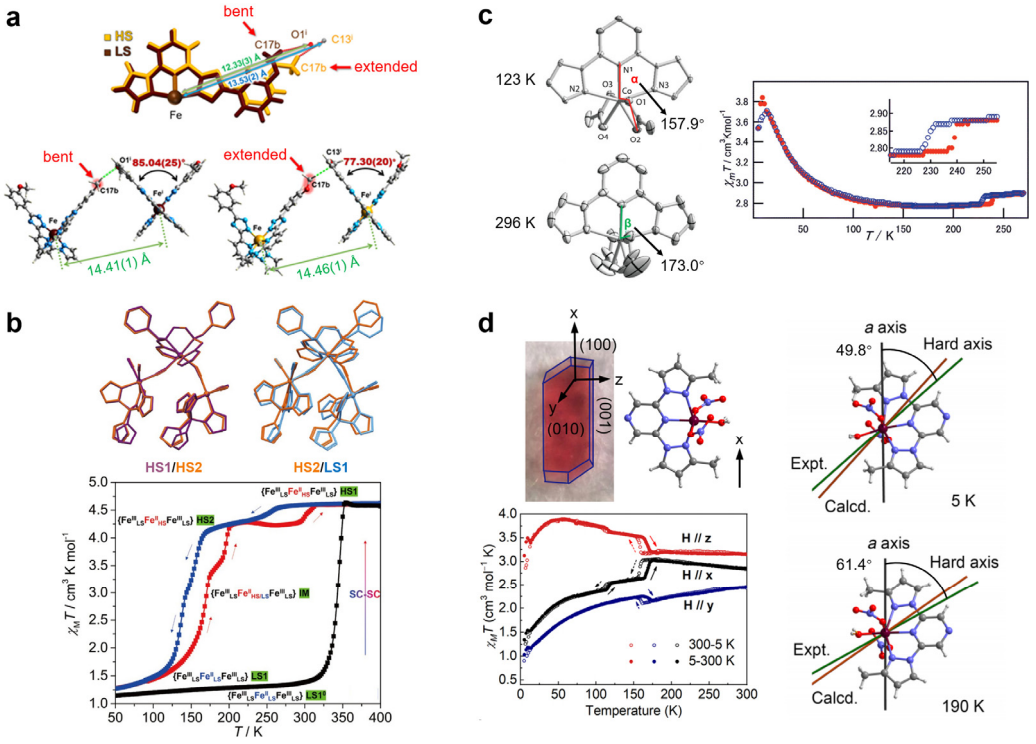

Figure 4. (**a**) **Top**: the overlapping diagram of [Fe^{II}(2-(5-(3-methoxy-4*H*-1,2,4-triazol-3-yl)-6-(1*H*-pyrazol-1-yl))pyridine)] between different spin states and the conformational change in the 3MeO group. **Bottom**: the influence of the conformation changes in the 3MeO group. Reproduced with permission from [52]. (**b**) Overlapping diagrams of the solvent-free complex {$Fe^{III}_2Fe^{II}$} between the different spin states and the temperature-dependent magnetic susceptibility for {$Fe^{III}_2Fe^{II}$}. Reproduced with permission from [53]. (**c**) **Left**: changes in molecular structure and the specific dihedral angle of [$Co(NO_3)_2$(2,6-di(pyrazol-1-yl)pyrazine)] before and after phase transition. **Right**: the abrupt step in the magnetic susceptibility around the phase transition critical temperature suggests the modulation of the orbital angular momentum due to the structural phase transition. Reproduced with permission from [54]. (**d**) **Left**: the schematic diagram of the test direction (*x*, *y* and *z*) in the single−crystal magnetic susceptibility measurement of [$Co(ONO_2)_2(H_2O)$(mprpz)] and the corresponding experimental value. **Right**: the magnetic anisotropy before and after phase transition. Reproduced with permission from [55].

In 2009, Yoshizawa and Sato et al. reported a high-spin cobalt(II) complex [$Co(NO_3)_2$(2,6-di(pyrazol-1-yl)pyrazine)] with magnetic bistability, in which two nitrate ligands adopt a symmetric bidentate coordination mode [54]. The complex undergoes structural changes, involving symmetry twisting and significant displacement of nitrate ligands (Figure 4c). According to DFT calculations, the thermal hysteresis of the magnetic susceptibility between 228 and 240 K occurs mainly due to the quenching of orbital angular momentum caused by the symmetry twisting of nitrate ligands. This is the first time to realize the magnetic multi-stability of transition metal complexes through orbital angular momentum quenching rather than controlling their spin states. Another work by Sato et al. was published in 2021 to modulate orbital angular momentum by using the rotation of water molecule ligands [55]. They reported that the orientation of the water molecule ligand in the complex [$Co(ONO_2)_2(H_2O)$(mprpz)] (mprpz = 2,6-bis(3-methylpyrazol-1-yl)pyrazine) is adjusted accordingly with the change in the position of the nitrate ligand to maintain the strongest hydrogen bond interactions. The structural phase transition results in the modulation of orbital angular momentum. The reversible rotational reorientation of equatorial coordinated water molecules can significantly affect the magnetic anisotropy through the metal–ligand π^* anti-bond interaction (Figure 4d). Especially when the water molecules rotate by 21.2 ± 0.2°, the directional susceptibility varies by about 30% along the crystal-

lographic *a*-axis. This work explored the effect of structural phase transition on magnetic anisotropy at the single crystal level for the first time.

In short, the thermal-induced motion of alkyl chains and non-alkyl groups as the dynamic parts of ligands may induce entropy-driven structural phase transition of the complexes, thus realizing the reversible control of magnetic properties. More importantly, by virtue of the thermo-reversibility of such structural phase transition, the switchable magnetic behavior could be repeated without fatigue, affording a potential route for high-performance magnetic multi-stable materials.

3. Thermal-Induced Dynamics of Counterions

Another promising strategy is to induce magnetic responses by the thermal-induced motion of counterions. The majority of works based on counterion motion are accompanied by order–disorder type phase transitions. There are three main kinds of order–disorder transitions: positional disordering in solids, directional disordering that can be static or dynamic, and disordering linked with electron and nuclear spin states [18]. Such phase transitions might modify the crystal lattice properties or symmetry, thus affecting the orbital angular momentum and, consequently, the magnetic properties. This section will be described in two parts: the countercations and the counteranions.

3.1. Countercations

In 2005, Saito and coworkers used complex $[Cs_2(18\text{-crown-}6)_3][Ni(dmit)_2]_2$ ($dmit^{2-}$ = 2-thioxo-1,3-dithiole-4,5-dithiolate) to study the interaction between the motion of the crown ether rotors of cylindrical supramolecular cations and electronic system [56]. The $[Ni(dmit)_2]^-$ ions ($S = 1/2$) form a π-dimer structure possessing a magnetic ground state sandwiched between the supramolecular cation layers, and the π-planes contact with the supramolecular cations. Above 220 K, the crown ethers of $Cs_2(18\text{-crown-}6)_3$ unit start to rotate. As the temperature increased, the occupancy of the two-fold disorder in 18-crown-6 gradually changed until it reached the same level at 300 K, and the rotation angle reached 30°. A significant deviation exists in fitting χ_M vs. T using the singlet-triplet thermal excitation model at high temperatures. This is due to the lattice modulation caused by the motion of crown ether, which induces the conformation of $[Ni(dmit)_2]^-$ slightly distorted and improves the intra-dimer transfer integral interaction as well as the magnetic exchange energy. This study illustrates the feasibility of manipulating the magnetic interactions of magnetic units in the solid state via molecular rotors in supramolecular cations.

Due to the advantages of structural tunability and versatility, considerable efforts have been devoted to creating novel metal–organic frameworks (MOFs) with advanced functionality [57]. Given that the structures of perovskite-type MOFs can be tuned by well-matched rigid cages and dynamic guest molecules, they can offer the exciting possibilities of building switchable materials. As a class of well-designed switchable molecular dielectrics, a series of perovskite-type (ABX_3) MOFs, $[(CH_3)_2NH_2][M(HCOO)_3]$ (M = Mn^{II}, Fe^{II}, Co^{II}, Ni^{II}, Zn^{II}) and $[(CH_3)_2NH_2][KCo(CN)_6]$ have attracted extensive attention. Both of these MOFs undergo reversible order–disorder phase transitions at critical temperatures [57–65]. According to these studies, it is the orientation of the polar $[(CH_3)_2NH_2]^+$ (dimethylammonium cation, DMA^+) under different temperatures that is responsible for this order–disorder phase transition.

Inspired by these works, a series of azido-bridged MOFs of the perovskite-type structure $[(CH_3)_nNH_{4-n}][Mn(N_3)_3]$ (n = 1~4) were synthesized by Wang et al. in 2013 [66]. They all have flexible lattices, which can not only accommodate cations of different sizes and shapes, but also adapt to structural phase transitions generated at different temperatures. Interestingly, they also demonstrated the cation-dependent magnetic ordering in these MOFs. With the cation size increasing, the magnetic ordering temperature decreases in order, which means that there is stronger magnetic coupling in the denser structure. Due to the antiferromagnetic coupling transmitted by the azide bridges, the $\chi_M T$ values of all complexes at high temperature are smaller than the expected spin-only value for an

isolated Mn^{II} ion. Thermal magnetic hysteresis near room temperature is observed in these complexes, which is the result of modification of the magnetic coupling caused by the order–disorder phase transition. In fact, the authors believe that the driving force of this phase transition is not obvious. They speculate that it may be related to the N-H···N hydrogen bonds formed by $[(CH_3)_nNH_{4-n}]^+$ cations and Mn^{II}-N_3^- network and the symmetry of cations, which allows the exploration of different cations in the future to construct novel magnetic bistable materials. These results have indicated that introducing flexible or polar moieties undergoing order–disorder transition into complexes may lead to switchable magnetic and dielectric properties, and even more diverse functionality.

Because ferroelectricity and magnetism are mutually exclusive in a single phase, it is difficult to obtain multiferroic substances (referring to materials with two or three different switchable ferroic orders, that is, ferromagnetism, ferroelectricity and ferroelasticity) [67]. This is because ferroelectrics need empty d-shells of transition-metal ions, while magnetic materials need partially filled d-shells [68]. Xiong and coworkers proposed the first organic–inorganic hybrid multiferroic complex $[(CH_3CH_2)_3(CH_3)N][FeBr_4]$ in 2012, which shows strong magnetodielectric coupling above room temperature (Figure 5a) [67]. The complex undergoes a first-order structural phase transition from ferroelectric (polar space group $P6_3mc$) to paraelectric (centrosymmetry) phase, which is caused by the disorder of cations at ca. 360 K. This process is accompanied not only by significant dielectric anomalies but also reversible magnetic phase transitions, which may be attributed to orbital angular momentum modulation, resulting in strong magnetodielectric (MD) coupling. This work provides guidance for exploring molecule-based materials with magnetodielectric coupling effect and developing multiferroic materials.

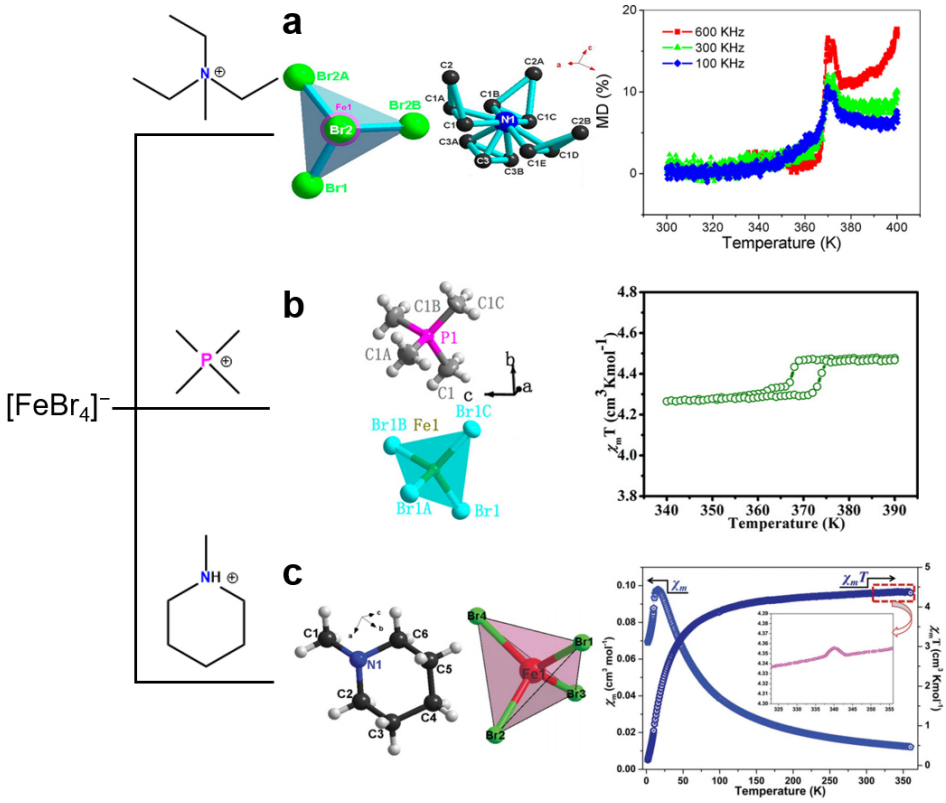

Figure 5. Inorganic–organic hybrid complexes composed of $[FeBr_4]^-$ anions and various cations, and their magnetic properties. (**a**) Molecular structure and temperature−dependent magnetodielectric properties of $[(CH_3CH_2)_3(CH_3)N][FeBr_4]$. Reproduced with permission from [67]. (**b**) Molecular structure and temperature−dependent magnetic susceptibility of $[(CH_3)_4P][FeBr_4]$. Reproduced with permission from [68]. (**c**) Molecular structure and temperature−dependent magnetic susceptibility of $[C_6H_{14}N][FeBr_4]$. Reproduced with permission from [69].

Another work of this group with multiferroic properties is the two inorganic–organic hybrid complexes $[(CH_3)_4P][FeCl_4]$ and $[(CH_3)_4P][FeBr_4]$, which display the coexistence of switchable dielectric, magnetic and optical responses (Figure 5b) [68]. Similarly, both complexes exhibit dielectric anomalies that can be tuned in three dielectric states and switchable second harmonic generation (SHG) effects, corresponding to continuous reversible temperature-triggered phase transitions above room temperature. The complex $[(CH_3)_4P][FeBr_4]$ not only exhibits a stronger antiferromagnetic interaction, but also shows an obvious magnetic phase transition with a thermal hysteresis of 6 K due to the quenching of orbital angular momentum, which does not exist in $[(CH_3)_4P][FeCl_4]$. This work concludes that the major reason for the phase transitions in both complexes is derived from the thermally actuated rotation of $[(CH_3)_4P]^+$ cations.

Three years later, Luo and coworkers demonstrated dielectric bistability and magnetic response in a similar inorganic–organic hybrid complex, N-methylpiperidinium tetrabromoferrate(III) $[C_6H_{14}N][FeBr_4]$ (Figure 5c) [69]. This complex undergoes a symmetry-breaking phase transition at ca. 340 K. Correspondingly, the space group of this crystal transforms from $P2_1/c$ at room temperature into *Cmcm*. Strikingly, the complex displays switchable dielectric activities. In addition, a weak magnetic anomaly is observed near the phase transition point in the magnetic susceptibility measurement. Like $[(CH_3)_4P][FeCl_4]$, the phase transition is closely relevant to the order–disordering of organic cations. It is worth mentioning that even though organic cations are highly disordered at high temperature, the framework remains in order. This further confirms the indispensable role of combining flexible and stable components in such dynamic crystals. Consequently, such a novel class of hybrid complexes has shown great potential as promising multifunctional materials.

3.2. Counteranions

A typical example is the order–disorder structural phase transition and the accompanying mechanical response at the macroscopic level triggered by the thermal motion of oxalate anions. In 2014, Sato and coworkers determined that the ox^{2-} anion in complex $[Ni(en)_3](ox)$ (en = ethylenediamine, ox^{2-} = oxalate dianion) would undergo reversible rotation reorientation (90°) with the change in temperature (Figure 6a). The disappearance/appearance of the crystallographic three-fold axis caused by its order/disorder will lead to symmetry-breaking ($P2_1/n \leftrightarrow P-31c$) [70]. The rotational reorientation of ox^{2-} leads to an increase in the Ni···Ni distance along the crystallographic *c*-axis, and transfers rapidly in the crystal through the cooperative movement of N-H···O hydrogen bonds around the anions. Thus, the significant expansion and contraction of the crystal are observed at the macroscopic scale (corresponding to a change of approximately 5% in the length of the *c*-axis). Based on this study, the authors replaced the metal center with divalent cobalt, which is prone to modulation of orbital angular momentum.

An analogue complex $[Co(en)_3](ox)$ was reported in 2017, and a similar reversible rotation reorientation of 90° of ox^{2-} anions and a change in crystal shape were observed [71]. From the high-temperature phase to the low-temperature phase, the symmetry-breaking (the space group changes from $P-31c$ to $P-1$) occurs in the Co^{II} complex, suggesting a ferroelastic phase transition. Near the phase transition temperature, the magnetic susceptibilities measured perpendicular to and parallel to the long axis of the crystal exhibit abrupt changes of 2% and 12% respectively, which implies the magnetic susceptibility of the single crystal is anisotropic and demonstrates the modulation of orbital angular momentum (Figure 6b). This is due to the loss of the C_3-axis of the $[Co(en)_3]^{2+}$ cations in the low-temperature phase accompanied by the slight distortion of the ideal D_3 coordination environment of the Co^{II} ions, which directly affects the orientation of the magnetic anisotropy.

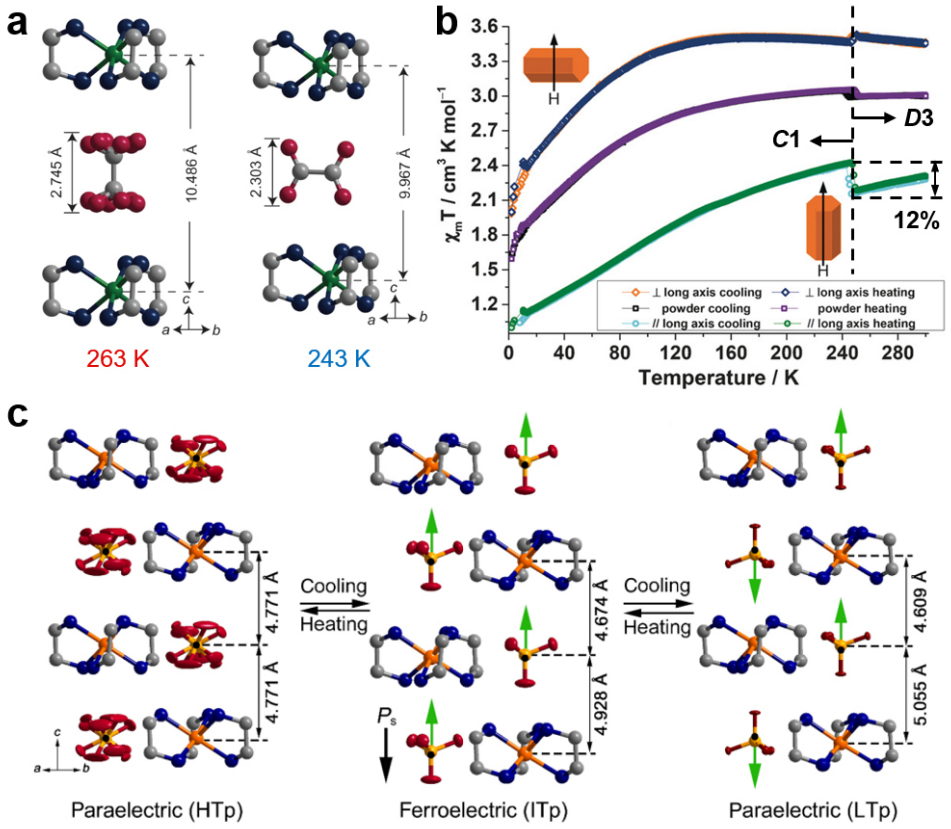

Figure 6. (**a**) The rotation of oxalate dianion for $[Ni(en)_3](ox)$ and the change in distance between Ni^{2+} ions before and after phase transition. Reproduced with permission from [70]. (**b**) Variable temperature−dependent magnetic susceptibilities of single−crystal and powdered samples of $[Co(en)_3](ox)$. Reproduced with permission from [71]. (**c**) Packing diagrams of $[Co(en)_3](SO_4)$ in the different phases. With the change in temperature, sulfate dianions show gradual ordering/disordering. Reproduced with permission from [72].

Not satisfied with the ferroelastic phase transition in $[Co(en)_3](ox)$, Yao et al. aim to manipulate the spin–orbit coupling of the transitionmetal magnetic center by introducing dynamic polarized anions so as to achieve cooperative switching of magnetic and ferroelectric properties [72]. During the cooling process, the complex $[Co(en)_3](SO_4)$ achieves a paraelectric–ferroelectric–paraelectric phase transition (the space group changes from trigonal $P-31c$ at 185 K to polar trigonal $P31c$ at 160 K, and then to nonpolar $P-3$ at 140 K) through the gradual ordering of sulfate dianions (Figure 6c). The motion (including rotation and unidirectional displacement) of SO_4^{2-} causes the change in the coordination environment in the metal center through the strong synergistic interaction of abundant N−H···O hydrogen bonds, thus showing a reversible two-step magnetic switching behavior owing to orbital angular momentum modulation. The paraelectric–ferroelectric–paraelectric phase transition results from competing hydrogen bond and dipole–dipole interactions between $[Co(en)_3]^{2+}$ cations and SO_4^{2-} anions.

The order–disorder motions of counterions have the potential to cause tiny changes in the coordination geometry of the metal centers, resulting in crystallographic symmetry-breaking and the modulation of orbital angular momentum. Therefore, these works of entropy-driven order–disorder-type molecular rotors provide a promising strategy for the development of magnetic multi-stable materials, anisotropic magnetic switches, and even strong magnetoelectric coupling.

4. Thermal-Induced Dynamics of Coordination Number

Compared with the perturbation of the coordination environment of the metal centers through the dynamic structural changes, the more robust approach is to directly change the coordination number (C.N.) [73,74]. The reversible changes in coordination number can induce the transition of the spin state. In addition, the energy levels of the corresponding d-orbitals can be adjusted, resulting in a great change in the energy gap between the ground and the excited crystal-field terms, thus leading to significant modulation of the orbital angular momentum [54,75,76].

In 2007, using a typical iron complex, $[Fe^{II}L(CN)_2]\cdot H_2O$ (L = 2,13-dimethyl-6,9-dioxa-3,12,18-triazabicyclo[12.3.1]octadeca-1(18),2,12,14,16-pentaene), Guionneau et al. demonstrated a reversible thermal-induced modification of the metal coordination number in the solid state and associated with a spin crossover at 155 K [76]. The metal center undergoes a structural phase transition from the 7-coordinate ($N_3C_2O_2$) HS state to the 6-coordinate (N_3C_2O) LS state, accompanied by a molecular volume change of ca. 40%. The significance of such non-destructive reversible metal–ligand bond breakage and formation in solid phase transition is revealed for the first time.

In 2019, Murrie et al. studied the single-crystal-to-single-crystal phase transition of single ion magnet (SIM) $[Co^{II}(NO_3)_3(H_2O)(HDABCO)]$ (DABCO = 1,4-diazabicyclo[2,2,2]octane) [77]. The axial coordination atoms are a nitrogen atom from protonated $[HDABCO]^+$ and an oxygen atom from H_2O, respectively. The reversible change in coordination number (C.N. = 5 or 7) is attributed to the thermal-induced dynamic structural change in NO_3^- at the equatorial plane (Figure 7a). Because the nitrate at the N5 position, one of the three monodentate NO_3^- (η^1-ONO_2) ligands, exhibits disorder between two different positions, the Co^{II} complex has a mixed coordination environment (75~95% trigonal bipyramidal and 25~5% vacant octahedron) at high-temperature phase. Upon cooling below 140 K, the nitrate at the N5 position becomes ordered, and the coordination mode along with the nitrate at the N4 position changes from monodentate to bidentate (η^2-ONOO). Meanwhile, the Co^{II} center adopts a 7-coordinate pentagonal bipyramidal coordination environment. The anomaly in the decreasing rate of variable–temperature magnetic susceptibilities between 140 and 160 K during cooling is related to the change in the coordination environment (Figure 7b). However, this phenomenon is not significant.

In 2020, Sato and coworkers also synthesized a divalent cobalt complex $[Co(NO_3)_2$(ethyl-2,6-di(1*H*-pyrazol-1-yl)isonicotinate)] by thermally induced modulating the mono/bidentate coordination mode of NO_3^- ligands, i.e., dynamic bond approach (Figure 8a) [75]. With the change in coordination number (C.N. = 6 or 7), the variation in the $\chi_M T$ value on the powdered sample is 10.0~11.0% with a thermal hysteresis of 14 K (Figure 8b). The variation value along the easy axis for the oriented sample even increases up to 20%. A plausible explanation for these phenomena is that the breaking and reformation of the Co−O coordination bond effectively adjust the increase and decrease in the energy of the first singly occupied d-orbital. The significant change in the energy gap between the excited and ground states leads to a significant quenching and restoration of orbital angular momentum. Notably, this strategy of dynamic bond has realized the largest change in the modulation of orbital angular momentum reported to date.

The above studies reveal that the reversible changes in coordination number through thermal perturbation can effectively tune the magnetic properties of molecular magnetic materials, which provides a new pathway towards molecular memory and switching devices.

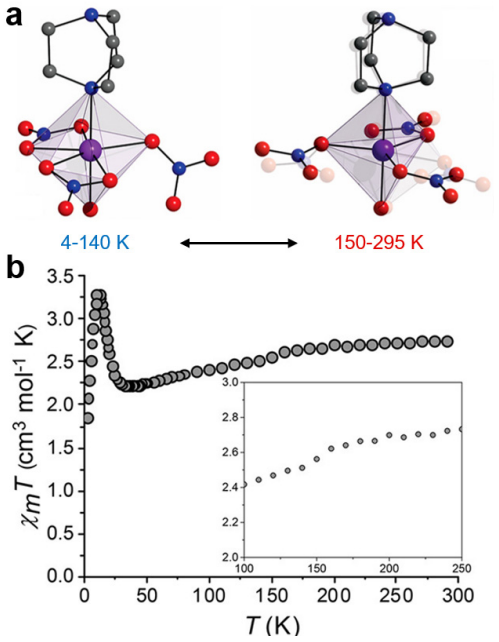

Figure 7. (**a**) Molecular structures of [$Co^{II}(NO_3)_3(H_2O)$(HDABCO)] in the different phases. The dynamic structure change in nitrate causes the reversible switching of the coordination number of the Co^{II} metal center. Color codes: gray (C), blue (N), red (O), and purple (Co^{II}). (**b**) Variable−temperature dependent magnetic susceptibility of the complex. Inset: the weak anomaly between 140 and 160 K.Reproduced with permission from [77].

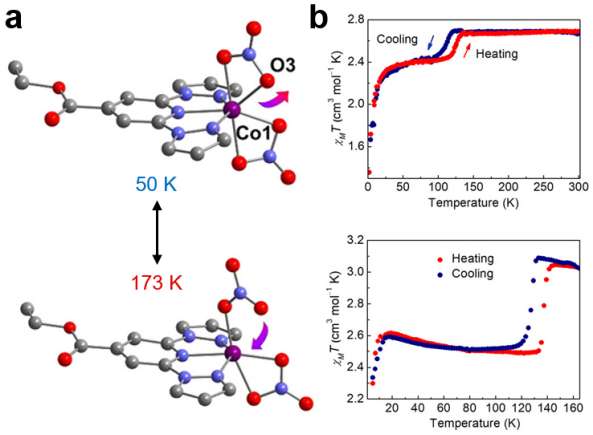

Figure 8. (**a**) Complex [$Co(NO_3)_2$(ethyl-2,6-di(1*H*-pyrazol-1-yl)isonicotinate)] realizes the reversible switching of the coordination number (C.N. = 6 or 7) of the Co^{II} metal center through the motion of the nitrate. Color codes: gray (C), blue (N), red (O), and purple (Co^{II}). (**b**) Temperature−dependent magnetic susceptibility of the powdered sample (**top**) and along the magnetic easy axis for the oriented sample (**bottom**). Reproduced with permission from [75].

5. Thermal-Induced Dynamics of Neutral Guests

Many studies mentioned above have shown that introducing polar or flexible components into molecular magnetic materials can induce first-order phase transitions, thus generating novel multifunctional responses. Introducing the concept of AMMs into the design of molecular magnetic materials can trigger the dynamic spatiotemporal changes in chemical and electronic structures under the external stimuli, thereby generating the synergistic modulation of molecular structure and magnetoelectric properties and realizing the output of physical properties [78]. Structurally flexible crown ethers, which can act as the rotators of molecular rotors in the order–disorder-type phase transition, are one of

the important building units in the field of AMMs and powerful candidates for precisely controlling magnetism through external stimuli. However, according to the existing reports, crown ethers and their derivatives are usually used to build supramolecular cations with alkali metals, amines, pyridiniums and oxoniums, while few works used neutral crown ethers to construct rotor units [56,79–87]. Therefore, to manipulate the magnetoelectric properties, taking good advantage of supramolecular interaction between the neutral crown ether guest and the metal–ligand complex has broad prospects.

Based on the tactic mentioned above, Liu et al. recently selected the flexible 18-crown-6 molecule and the Co^{II} ion with Jahn–Teller effect to accurately design and synthesize an order–disorder-type phase transition complex $[Co(NCS)_2(H_2O)_2(4\text{-amino-3-chloropyridine})_2]\cdot(18\text{-crown-6})$ (Figure 9a) [78]. Crystallographic data show that "R_w–S–R_w" (where R_w is the rotating water molecule and the S is the "stator" Co^{II}) fragment and the guest 18-crown-6 rotator (denoted as R_c) assemble into "$R_c\cdots R_w$–S–$R_w\cdots R_c$" type supramolecular one-dimensional chain through intermolecular hydrogen bonds. There are no counterion "stator" fragments for charge balancing. The complex exhibits a reversible switch of Jahn–Teller axis and thermally induced rotation of the 18-crown-6 rotor near room temperature. The thermally activated intermolecular motion of crown ethers and coordination water molecules is the key to triggering a single-crystal-to-single-crystal first-order phase transition with $T_{\uparrow}$ = 282 K and $T_{\downarrow}$ = 276 K. After changing from the low-temperature phase to the high-temperature phase, the single-crystal angular-resolved magnetometry measurement showed that the easy axis and the hard axis rotate by 14.6° and 14.1°, respectively, indicating that the magnetic anisotropy has changed significantly before and after phase transition (Figure 9a).

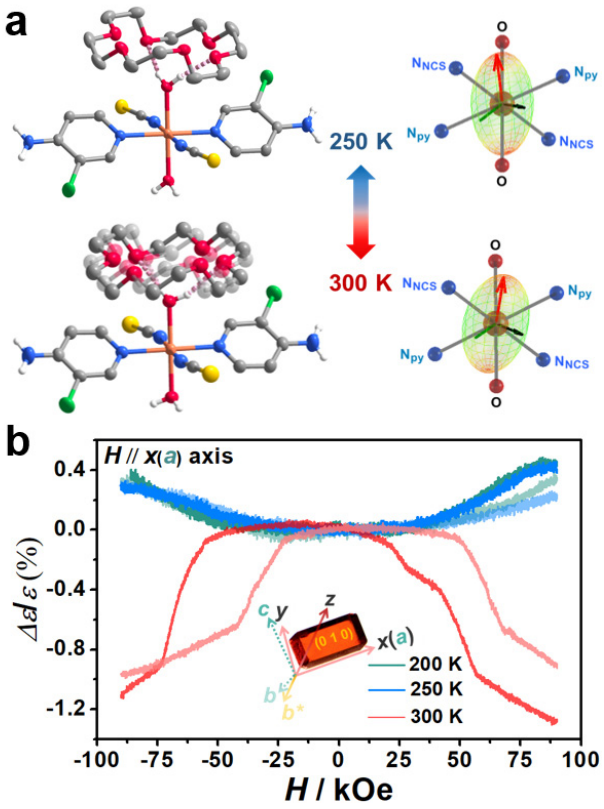

Figure 9. (**a**) The changes in molecular structure and magnetic anisotropy of $[Co(NCS)_2(H_2O)_2(4\text{-amino-3-chloropyridine})_2]\cdot(18\text{-crown-6})$ before and after phase transition. Color codes: white (H), gray (C), blue (N), red (O), yellow (S), green (Cl) and orange (Co^{II}). (**b**) Single−crystal magnetodielectric effect with the magnetic field applied in crystallographic *a* axis direction. Reproduced with permission from [78].

In addition, in recent years, inorganics have occupied the main part of single-phase magnetodielectric materials [88–91], but few works of molecular magnets have been found [67,92–98]. Among them, most of the molecular magnets exhibit positive magnetodielectric effect. For example, the first organic–inorganic hybrid multiferroic complex $[(CH_3CH_2)_3(CH_3)N][FeBr_4]$ mentioned above in the section of "Counterions" shows a large MD ratio (ca. 18%) at 600 kHz [65]. Additionally, the MD ratio of alkylated Co^{II} complex, which exhibits the co-occurrence of liquid crystal, ferroelectric, and field-induced single molecular magnet properties, is even as high as 83.4% [98]. Nevertheless, the complex $[Co(NCS)_2(H_2O)_2(4\text{-amino-3-chloropyridine})_2]\cdot(18\text{-crown-6})$ shows an ON/OFF negative magnetodielectric effect in the high-temperature/low-temperature phases, respectively, suggesting that the rotation of 18-crown-6 and coordination water molecules may lead to a stronger spin–lattice interaction in the high-temperature phase (Figure 9b).

There are two highlights in this work: (1) Inspired by the similarities between AMMs and switchable magnetic materials, the crown ether rotor was introduced as a neutral guest to realize the reversible switching of magnetoelectric properties. (2) The synergistic modulation of the magnetic anisotropy and magnetodielectric effects in magnetic molecular solids was accomplished for the first time.

6. Summary and Perspective

We have described recent advances in switchable magnetic complexes whose magnetic properties are remarkably modulated under external thermal stimuli. This is achieved by structural phase transition rather than conventional spin crossover or charge transfer. This review summarizes four types of thermal-induced dynamic structural changes, which occur in flexible ligands, counterions, coordination numbers and neutral guests, respectively. Essentially, temperature-sensitive tunable structural moieties are introduced to induce reversible structural phase transitions in the crystal, thus potentially achieving magnetic bistability accompanied by thermal hysteresis.

Although switchable magnetic properties modulated by dynamic structural changes have been demonstrated in many of the aforementioned studies, the limitations and challenges of this method still exist. Hence, we attempt to put forward some perspectives here to foster the development of functional magnetic materials.

(1) One of the most important goals of magnetic switches is to achieve wide thermal hysteresis centered at room temperature. This means that both states can be accessible at the same temperature for such materials. The thermal hysteresis width varies greatly among the complexes with thermal-induced phase transitions summarized herein (Table 1). Apparently, the modulation of the orbital angular momentum is usually accompanied by a narrower thermal hysteresis compared to those of the spin transition. The thermal hysteresis of [Fe^{II}(2-(5-(3-methoxy-4*H*-1,2,4-triazol-3-yl)-6-(1*H*-pyrazol-1-yl))pyridine)] can even reach 105 K, which is not inferior to the conventional SCO complexes with large hysteresis [99–102]. This demonstrates the potential of flexible complexes that can undergo structural phase transitions. The supramolecular interactions (hydrogen bonding, $\pi\cdots\pi$ stacking, etc.) may have an important influence on the intermolecular cooperative effect, which in turn can regulate the phase transition temperature as well as the thermal hysteresis width. As a result, when designing structural phase transition complexes, supramolecular cooperativity should be appropriately introduced and explored. However, the detailed mechanism has not yet been elucidated at present. A lot of exploration is still needed to achieve a deeper understanding by further realizing targeted design and synthesis.

(2) The reversible switching of coordination number is more pronounced to modulate the orbital contribution, and it has the potential to facilely construct the supramolecular structures by using neutral guests, since the neutral guests do not require compatible counterion fragments to compensate for the charge imbalance. However, there are few studies of these two types. To disrupt this scarcity, the tactics for designing these types need to be further explored.

(3) Likewise, the stimuli of light, electric or magnetic field may cause reversible changes in the crystal structure to regulate magnetic properties, thus providing research interest and promising applications in optical switches and magnetoelectric devices. Furthermore, apart from the sole control of heat, light and electric or magnetic field, it is wonderful to realize the response of a single moiety to multiple stimuli, as well as the cooperative response of multiple moieties to multiple stimuli.

(4) Finally, the precise design of materials with switchable magnetic characteristics is still challenging. To guide the development of high-performance functional materials, it is necessary to have a deeper understanding of the roles between crystal structures and structural phase transition, as well as magneto-structural correlation. More importantly, designing and realizing multifunctional materials with strong synergistic effects between magnetic, electric, fluorescent, and other physical properties is very helpful.

Table 1. Transition temperature and their thermal hysteresis (related to structural phase transition) from magnetic susceptibility for the selected complexes discussed in this review.

Complex	$T_{\downarrow}$/K	$T_{\uparrow}$/K	ΔT/K	Comment	Ref.
$[Co^{II}(C_{14}\text{-terpy})_2](BF_4)_2$	250	307	57		[43]
$[Co^{II}(C_{16}\text{-terpy})_2](BF_4)_2$	217	260	43		[43]
$[Co^{II}(C_{14}\text{-terpy})_2](BF_4)_2\cdot$MeOH	184	206	22		[46]
$[Fe^{II}(n\text{Bu-im})_3(\text{tren})](PF_6)_2$	115	129	14	Scan rate: 4 K min^{-1}	[48]
	135	176	41	Scan rate: 0.1 K min^{-1}	
$[Fe^{II}(C_{10}\text{-pbh})_2]$	–	ca. 298	1.2		[49]
$[Fe^{II}$(2-(5-(3-methoxy-4*H*-1,2,4-triazol-3-yl)-6-(1*H*-pyrazol-1-yl))pyridine)]	255	360	105		[52]
$\{[(\text{pzTp})Fe^{III}(CN)_3]_2[Fe^{II}(L)]\}$	256	300	44	0.5 or 1 K min^{-1} Scan-rate dependence	[53]
$[Co^{II}(NO_3)_2$(2,6-di(pyrazol-1-yl)pyrazine)]	228	240	12		[54]
$[Co^{II}(ONO_2)_2(H_2O)(\text{mprpz})]$	–	ca. 110	7	Low-temperature phase ↔ intermediate phase	[55]
	155	165	10	Intermediate phase ↔ high-temperature phase	
$[CH_3NH_3][Mn^{II}(N_3)_3]$	264	277	13		[66]
$[(CH_3)_2NH_2][Mn^{II}(N_3)_3]$	286	298	12		
$[(CH_3)_3NH][Mn^{II}(N_3)_3]$	363	356	7		
$[(CH_3)_4N][Mn^{II}(N_3)_3]$	305	309	4		
$[(CH_3CH_2)_3(CH_3)N][Fe^{III}Br_4]$	361	366	5		[67]
$[(CH_3)_4P][Fe^{III}Br_4]$	368	374	6		[68]
$[Co^{II}(en)_3](ox)$	–	ca. 250	4		[71]
$[Co^{II}(en)_3](SO_4)$	–	ca. 177	4		[72]
$[Co^{II}(NO_3)_2$(ethyl-2,6-di(1*H*-pyrazol-1-yl)isonicotinate)]	–	ca. 128.5	14		[75]
$[Co^{II}(NCS)_2(H_2O)_2$(4-amino-3-chloropyridine)$_2]\cdot$(18-crown-6)	277.6	281.2	3.6		[78]

Magnetic memory and switching devices fabricated from multi-stable materials can convert external signals into useful output signals and perform related tasks. However, this field is still in its infancy, which presents ample opportunities for their design. The control of dynamic structural change provides a feasible and promising strategy for modulating

the magnetic properties of molecular solids and the development of switchable devices. In order to achieve this, chemists will need to make great efforts in the future.

Author Contributions: Writing—original draft preparation, S.-N.D. and C.-Y.Y.; writing—review and editing, S.-N.D. and J.-L.L.; supervision, M.-L.T. and J.-L.L. All authors have read and agreed to the published version of the manuscript.

Funding: This research was funded by the National Key Research and Development Program of China (No. 2018YFA0306001), the National Natural Science Foundation of China (Nos. 21821003 and 22073115), the Pearl River Talent Plan of Guangdong (No. 2017BT01C161), and Science and Technology Projects in Guangzhou (202201011095).

Institutional Review Board Statement: Not applicable.

Informed Consent Statement: Not applicable.

Data Availability Statement: Not applicable.

Conflicts of Interest: The authors declare no conflict of interest.

References

1. Gütlich, P.; Hauser, A.; Spiering, H. Thermal and Optical Switching of Iron(II) Complexes. *Angew. Chem. Int. Ed. Engl.* **1994**, *33*, 2024–2054. [CrossRef]
2. Coronado, E. Molecular magnetism: From chemical design to spin control in molecules, materials and devices. *Nat. Rev. Mater.* **2020**, *5*, 87–104. [CrossRef]
3. Ni, Z.P.; Liu, J.L.; Hoque, M.N.; Liu, W.; Li, J.Y.; Chen, Y.C.; Tong, M.L. Recent advances in guest effects on spin-crossover behavior in Hofmann-type metal-organic frameworks. *Coord. Chem. Rev.* **2017**, *335*, 28–43. [CrossRef]
4. Zhao, L.; Meng, Y.S.; Liu, Q.; Sato, O.; Shi, Q.; Oshio, H.; Liu, T. Switching the magnetic hysteresis of an [Fe^{ii}–NC–W^{v}]-based coordination polymer by photoinduced reversible spin crossover. *Nat. Chem.* **2021**, *13*, 698–704. [CrossRef] [PubMed]
5. Ohkoshi, S.i.; Imoto, K.; Tsunobuchi, Y.; Takano, S.; Tokoro, H. Light-induced spin-crossover magnet. *Nat. Chem.* **2011**, *3*, 564–569. [CrossRef] [PubMed]
6. Muñoz, M.C.; Real, J.A. Thermo-, piezo-, photo- and chemo-switchable spin crossover iron(II)-metallocyanate based coordination polymers. *Coord. Chem. Rev.* **2011**, *255*, 2068–2093. [CrossRef]
7. Bousseksou, A.; Molnár, G.; Salmon, L.; Nicolazzi, W. Molecular spin crossover phenomenon: Recent achievements and prospects. *Chem. Soc. Rev.* **2011**, *40*, 3313–3335. [CrossRef] [PubMed]
8. Brooker, S. Spin crossover with thermal hysteresis: Practicalities and lessons learnt. *Chem. Soc. Rev.* **2015**, *44*, 2880–2892. [CrossRef]
9. Halcrow, M.A. (Ed.) *Spin-Crossover Materials: Properties and Applications*; John Wiley & Sons: Hoboken, NJ, USA, 2013.
10. Heersche, H.B.; de Groot, Z.; Folk, J.A.; van der Zant, H.S.J.; Romeike, C.; Wegewijs, M.R.; Zobbi, L.; Barreca, D.; Tondello, E.; Cornia, A. Electron Transport through Single Mn_{12} Molecular Magnets. *Phys. Rev. Lett.* **2006**, *96*, 206801. [CrossRef]
11. Tyagi, P.; Riso, C. Magnetic force microscopy revealing long range molecule impact on magnetic tunnel junction based molecular spintronics devices. *Org. Electron.* **2019**, *75*, 105421. [CrossRef]
12. Dei, A.; Gatteschi, D.; Sangregorio, C.; Sorace, L. Quinonoid Metal Complexes: Toward Molecular Switches. *Acc. Chem. Res.* **2004**, *37*, 827–835. [CrossRef] [PubMed]
13. Tezgerevska, T.; Alley, K.G.; Boskovic, C. Valence tautomerism in metal complexes: Stimulated and reversible intramolecular electron transfer between metal centers and organic ligands. *Coord. Chem. Rev.* **2014**, *268*, 23–40. [CrossRef]
14. Sato, O.; Tao, J.; Zhang, Y.Z. Control of Magnetic Properties through External Stimuli. *Angew. Chem. Int. Ed.* **2007**, *46*, 2152–2187. [CrossRef]
15. Sato, O. Dynamic molecular crystals with switchable physical properties. *Nat. Chem.* **2016**, *8*, 644–656. [CrossRef]
16. Yao, Z.S.; Tang, Z.; Tao, J. Bistable molecular materials with dynamic structures. *Chem. Commun.* **2020**, *56*, 2071–2086. [CrossRef] [PubMed]
17. Binder, K. Theory of first-order phase transitions. *Rep. Prog. Phys.* **1987**, *50*, 783. [CrossRef]
18. Zhang, W.; Xiong, R.G. Ferroelectric Metal–Organic Frameworks. *Chem. Rev.* **2012**, *112*, 1163–1195. [CrossRef]
19. Cowley, R.A. Structural phase transitions I. Landau theory. *Adv. Phys.* **1980**, *29*, 13–59. [CrossRef]
20. Müller, U. *Symmetry Relations at Phase Transitions*; Oxford University Press: New York, NY, USA, 2013; pp. 196–215.
21. Clarke, J.B.; Hastie, J.W.; Kihlborg, L.H.E.; Metselaar, R.; Thackeray, M.M. Definitions of terms relating to phase transitions of the solid state (IUPAC Recommendations 1994). *Pure Appl. Chem.* **1994**, *66*, 577–594. [CrossRef]
22. Shi, C.; Han, X.B.; Zhang, W. Structural phase transition-associated dielectric transition and ferroelectricity in coordination compounds. *Coord. Chem. Rev.* **2019**, *378*, 561–576. [CrossRef]
23. Benelli, C.; Gatteschi, D. *Introduction to Molecular Magnetism: From Transition Metals to Lanthanides*; Wiley-VCH Verlag GmbH & Co. KGaA: Weinheim, Germany, 2015.
24. Gao, S. (Ed.) *Molecular Nanomagnets and Related Phenomena*; Springer: Berlin/Heidelberg, Germany, 2014.

25. Boča, R. Zero-field splitting in metal complexes. *Coord. Chem. Rev.* **2004**, *248*, 757–815. [CrossRef]
26. Gomez-Coca, S.; Cremades, E.; Aliaga-Alcalde, N.; Ruiz, E. Mononuclear Single-Molecule Magnets: Tailoring the Magnetic Anisotropy of First-Row Transition-Metal Complexes. *J. Am. Chem. Soc.* **2013**, *135*, 7010–7018. [CrossRef] [PubMed]
27. Novikov, V.V.; Pavlov, A.A.; Nelyubina, Y.V.; Boulon, M.-E.; Varzatskii, O.A.; Voloshin, Y.Z.; Winpenny, R.E.P. A Trigonal Prismatic Mononuclear Cobalt(II) Complex Showing Single-Molecule Magnet Behavior. *J. Am. Chem. Soc.* **2015**, *137*, 9792–9795. [CrossRef]
28. Yang, J.; Zhao, X.H.; Deng, Y.F.; Zhang, X.Y.; Chang, X.Y.; Zheng, Z.; Zhang, Y.Z. Azido-Cyanide Mixed-Bridged Fe^{III}–Ni^{II} Complexes. *Inorg. Chem.* **2020**, *59*, 16215–16224. [CrossRef]
29. Zadrozny, J.M.; Xiao, D.J.; Atanasov, M.; Long, G.J.; Grandjean, F.; Neese, F.; Long, J.R. Magnetic blocking in a linear iron(I) complex. *Nat. Chem.* **2013**, *5*, 577–581. [CrossRef] [PubMed]
30. Yao, X.N.; Du, J.Z.; Zhang, Y.Q.; Leng, X.B.; Yang, M.W.; Jiang, S.D.; Wang, Z.X.; Ouyang, Z.W.; Deng, L.; Wang, B.W.; et al. Two-Coordinate Co(II) Imido Complexes as Outstanding Single-Molecule Magnets. *J. Am. Chem. Soc.* **2017**, *139*, 373–380. [CrossRef] [PubMed]
31. Kassem, S.; van Leeuwen, T.; Lubbe, A.S.; Wilson, M.R.; Feringa, B.L.; Leigh, D.A. Artificial molecular motors. *Chem. Soc. Rev.* **2017**, *46*, 2592–2621. [CrossRef]
32. Coskun, A.; Banaszak, M.; Astumian, R.D.; Stoddart, J.F.; Grzybowski, B.A. Great expectations: Can artificial molecular machines deliver on their promise? *Chem. Soc. Rev.* **2012**, *41*, 19–30. [CrossRef]
33. Browne, W.R.; Feringa, B.L. Making molecular machines work. *Nat. Nanotechnol.* **2006**, *1*, 25–35. [CrossRef]
34. Erbas-Cakmak, S.; Leigh, D.A.; McTernan, C.T.; Nussbaumer, A.L. Artificial Molecular Machines. *Chem. Rev.* **2015**, *115*, 10081–10206. [CrossRef]
35. Moulin, E.; Faour, L.; Carmona-Vargas, C.C.; Giuseppone, N. From Molecular Machines to Stimuli-Responsive Materials. *Adv. Mater.* **2020**, *32*, 1906036. [CrossRef] [PubMed]
36. van Dijk, L.; Tilby, M.J.; Szpera, R.; Smith, O.A.; Bunce, H.A.P.; Fletcher, S.P. Molecular machines for catalysis. *Nat. Rev. Chem.* **2018**, *2*, 0117. [CrossRef]
37. Aprahamian, I. The Future of Molecular Machines. *ACS Cent. Sci.* **2020**, *6*, 347–358. [CrossRef] [PubMed]
38. Wang, Q.L.; Southerland, H.; Li, J.R.; Prosvirin, A.V.; Zhao, H.; Dunbar, K.R. Crystal-to-Crystal Transformation of Magnets Based on Heptacyanomolybdate(III) Involving Dramatic Changes in Coordination Mode and Ordering Temperature. *Angew. Chem. Int. Ed.* **2012**, *51*, 9321–9324. [CrossRef]
39. Zheng, T.; Clemente-Juan, J.M.; Ma, J.; Dong, L.; Bao, S.S.; Huang, J.; Coronado, E.; Zheng, L.M. Breathing Effect in a Cobalt Phosphonate upon Dehydration/Rehydration: A Single-Crystal-to-Single-Crystal Study. *Chem. Eur. J.* **2013**, *19*, 16394–16402. [CrossRef]
40. Fan, K.; Xu, F.; Kurmoo, M.; Huang, X.D.; Liao, C.H.; Bao, S.S.; Xue, F.; Zheng, L.M. Metal–Metalloligand Coordination Polymer Embedding Triangular Cobalt–Oxo Clusters: Solvent- and Temperature-Induced Crystal to Crystal Transformations and Associated Magnetism. *Inorg. Chem.* **2020**, *59*, 8935–8945. [CrossRef] [PubMed]
41. Galyametdinov, Y.; Ksenofontov, V.; Prosvirin, A.; Ovchinnikov, I.; Ivanova, G.; Gütlich, P.; Haase, W. First Example of Coexistence of Thermal Spin Transition and Liquid-Crystal Properties. *Angew. Chem. Int. Ed.* **2001**, *40*, 4269–4271. [CrossRef]
42. Fujigaya, T.; Jiang, D.L.; Aida, T. Switching of Spin States Triggered by a Phase Transition: Spin-Crossover Properties of Self-Assembled Iron(II) Complexes with Alkyl-Tethered Triazole Ligands. *J. Am. Chem. Soc.* **2003**, *125*, 14690–14691. [CrossRef]
43. Hayami, S.; Shigeyoshi, Y.; Akita, M.; Inoue, K.; Kato, K.; Osaka, K.; Takata, M.; Kawajiri, R.; Mitani, T.; Maeda, Y. Reverse Spin Transition Triggered by a Structural Phase Transition. *Angew. Chem. Int. Ed.* **2005**, *44*, 4899–4903. [CrossRef]
44. Zheng, J.; Kwak, K.; Xie, J.; Fayer, M.D. Ultrafast Carbon-Carbon Single-Bond Rotational Isomerization in Room-Temperature Solution. *Science* **2006**, *313*, 1951–1955. [CrossRef]
45. Sorai, M.; Saito, K. Alkyl chains acting as entropy reservoir in liquid crystalline materials. *Chem. Rec.* **2003**, *3*, 29–39. [CrossRef] [PubMed]
46. Hayami, S.; Murata, K.; Urakami, D.; Kojima, Y.; Akita, M.; Inoue, K. Dynamic structural conversion in a spin-crossover cobalt(ii) compound with long alkyl chains. *Chem. Commun.* **2008**, 6510–6512. [CrossRef] [PubMed]
47. Kobayashi, F.; Ohtani, R.; Nakamura, M.; Lindoy, L.F.; Hayami, S. Slow Magnetic Relaxation Triggered by a Structural Phase Transition in Long-Chain-Alkylated Cobalt(II) Single-Ion Magnets. *Inorg. Chem.* **2019**, *58*, 7409–7415. [CrossRef] [PubMed]
48. Seredyuk, M.; Muñoz, M.C.; Castro, M.; Romero-Morcillo, T.; Gaspar, A.B.; Real, J.A. Unprecedented Multi-Stable Spin Crossover Molecular Material with Two Thermal Memory Channels. *Chem. Eur. J.* **2013**, *19*, 6591–6596. [CrossRef] [PubMed]
49. Rosario-Amorin, D.; Dechambenoit, P.; Bentaleb, A.; Rouzières, M.; Mathonière, C.; Clérac, R. Multistability at Room Temperature in a Bent-Shaped Spin-Crossover Complex Decorated with Long Alkyl Chains. *J. Am. Chem. Soc.* **2018**, *140*, 98–101. [CrossRef]
50. Zhao, Q.; Xue, J.P.; Liu, Z.K.; Yao, Z.S.; Tao, J. Spin-crossover iron(ii) long-chain complex with slow spin equilibrium at low temperatures. *Dalton Trans.* **2021**, *50*, 11106–11112. [CrossRef] [PubMed]
51. Su, S.Q.; Kamachi, T.; Yao, Z.S.; Huang, Y.G.; Shiota, Y.; Yoshizawa, K.; Azuma, N.; Miyazaki, Y.; Nakano, M.; Maruta, G.; et al. Assembling an alkyl rotor to access abrupt and reversible crystalline deformation of a cobalt(II) complex. *Nat. Commun.* **2015**, *6*, 8810. [CrossRef] [PubMed]
52. Seredyuk, M.; Znovjyak, K.; Valverde-Muñoz, F.J.; da Silva, I.; Muñoz, M.C.; Moroz, Y.S.; Real, J.A. 105 K Wide Room Temperature Spin Transition Memory Due to a Supramolecular Latch Mechanism. *J. Am. Chem. Soc.* **2022**, *144*, 14297–14309. [CrossRef]

53. Zhao, X.H.; Shao, D.; Chen, J.T.; Gan, D.X.; Yang, J.; Zhang, Y.Z. A trinuclear $\{Fe^{III}{}_2Fe^{II}\}$ complex involving both spin and non-spin transitions exhibits three-step and wide thermal hysteresis. *Sci. China Chem.* **2022**, *65*, 532–538. [CrossRef]
54. Juhász, G.; Matsuda, R.; Kanegawa, S.; Inoue, K.; Sato, O.; Yoshizawa, K. Bistability of Magnetization without Spin-Transition in a High-Spin Cobalt(II) Complex due to Angular Momentum Quenching. *J. Am. Chem. Soc.* **2009**, *131*, 4560–4561. [CrossRef]
55. Su, S.Q.; Wu, S.Q.; Hagihala, M.; Miao, P.; Tan, Z.; Torii, S.; Kamiyama, T.; Xiao, T.; Wang, Z.; Ouyang, Z.; et al. Water-oriented magnetic anisotropy transition. *Nat. Commun.* **2021**, *12*, 2738. [CrossRef] [PubMed]
56. Akutagawa, T.; Shitagami, K.; Nishihara, S.; Takeda, S.; Hasegawa, T.; Nakamura, T.; Hosokoshi, Y.; Inoue, K.; Ikeuchi, S.; Miyazaki, Y.; et al. Molecular Rotor of Cs_2([18]crown-6)$_3$ in the Solid State Coupled with the Magnetism of [Ni(dmit)$_2$]. *J. Am. Chem. Soc.* **2005**, *127*, 4397–4402. [CrossRef]
57. Zhang, W.; Cai, Y.; Xiong, R.G.; Yoshikawa, H.; Awaga, K. Exceptional Dielectric Phase Transitions in a Perovskite-Type Cage Compound. *Angew. Chem. Int. Ed.* **2010**, *49*, 6608–6610. [CrossRef] [PubMed]
58. Wang, X.Y.; Gan, L.; Zhang, S.W.; Gao, S. Perovskite-like Metal Formates with Weak Ferromagnetism and as Precursors to Amorphous Materials. *Inorg. Chem.* **2004**, *43*, 4615–4625. [CrossRef] [PubMed]
59. Wang, Z.; Zhang, B.; Otsuka, T.; Inoue, K.; Kobayashi, H.; Kurmoo, M. Anionic NaCl-type frameworks of $[Mn^{II}(HCOO)_3{}^-]$, templated by alkylammonium, exhibit weak ferromagnetism. *Dalton. Trans.* **2004**, *4*, 2209–2216. [CrossRef]
60. Jain, P.; Dalal, N.S.; Toby, B.H.; Kroto, H.W.; Cheetham, A.K. Order−Disorder Antiferroelectric Phase Transition in a Hybrid Inorganic−Organic Framework with the Perovskite Architecture. *J. Am. Chem. Soc.* **2008**, *130*, 10450–10451. [CrossRef]
61. Jain, P.; Ramachandran, V.; Clark, R.J.; Zhou, H.D.; Toby, B.H.; Dalal, N.S.; Kroto, H.W.; Cheetham, A.K. Multiferroic Behavior Associated with an Order−Disorder Hydrogen Bonding Transition in Metal−Organic Frameworks (MOFs) with the Perovskite ABX3 Architecture. *J. Am. Chem. Soc.* **2009**, *131*, 13625–13627. [CrossRef]
62. Besara, T.; Jain, P.; Dalal, N.S.; Kuhns, P.L.; Reyes, A.P.; Kroto, H.W.; Cheetham, A.K. Mechanism of the order–disorder phase transition, and glassy behavior in the metal-organic framework $[(CH_3)_2NH_2]Zn(HCOO)_3$. *Proc. Natl. Acad. Sci. USA* **2011**, *108*, 6828–6832. [CrossRef]
63. Thomson, R.I.; Jain, P.; Cheetham, A.K.; Carpenter, M.A. Elastic relaxation behavior, magnetoelastic coupling, and order-disorder processes in multiferroic metal-organic frameworks. *Phys. Rev. B* **2012**, *86*, 214304. [CrossRef]
64. Fu, D.W.; Zhang, W.; Cai, H.L.; Zhang, Y.; Ge, J.Z.; Xiong, R.G.; Huang, S.D.; Nakamura, T. A Multiferroic Perdeutero Metal–Organic Framework. *Angew. Chem. Int. Ed.* **2011**, *50*, 11947–11951. [CrossRef]
65. Zhang, W.; Ye, H.Y.; Graf, R.; Spiess, H.W.; Yao, Y.F.; Zhu, R.Q.; Xiong, R.G. Tunable and Switchable Dielectric Constant in an Amphidynamic Crystal. *J. Am. Chem. Soc.* **2013**, *135*, 5230–5233. [CrossRef]
66. Zhao, X.H.; Huang, X.C.; Zhang, S.L.; Shao, D.; Wei, H.Y.; Wang, X.Y. Cation-Dependent Magnetic Ordering and Room-Temperature Bistability in Azido-Bridged Perovskite-Type Compounds. *J. Am. Chem. Soc.* **2013**, *135*, 16006–16009. [CrossRef] [PubMed]
67. Cai, H.L.; Zhang, Y.; Fu, D.W.; Zhang, W.; Liu, T.; Yoshikawa, H.; Awaga, K.; Xiong, R.G. Above-Room-Temperature Magnetodielectric Coupling in a Possible Molecule-Based Multiferroic: Triethylmethylammonium Tetrabromoferrate(III). *J. Am. Chem. Soc.* **2012**, *134*, 18487–18490. [CrossRef] [PubMed]
68. Shi, P.P.; Ye, Q.; Li, Q.; Wang, H.T.; Fu, D.W.; Zhang, Y.; Xiong, R.G. Novel Phase-Transition Materials Coupled with Switchable Dielectric, Magnetic, and Optical Properties: $[(CH_3)_4P][FeCl_4]$ and $[(CH_3)_4P][FeBr_4]$. *Chem. Mater.* **2014**, *26*, 6042–6049. [CrossRef]
69. Han, S.; Zhang, J.; Teng, B.; Ji, C.; Zhang, W.; Sun, Z.; Luo, J. Inorganic–organic hybrid switchable dielectric materials with the coexistence of magnetic anomalies induced by reversible high-temperature phase transition. *J. Mater. Chem. C* **2017**, *5*, 8509–8515. [CrossRef]
70. Yao, Z.S.; Mito, M.; Kamachi, T.; Shiota, Y.; Yoshizawa, K.; Azuma, N.; Miyazaki, Y.; Takahashi, K.; Zhang, K.; Nakanishi, T.; et al. Molecular motor-driven abrupt anisotropic shape change in a single crystal of a Ni complex. *Nat. Chem.* **2014**, *6*, 1079–1083. [CrossRef]
71. Yao, Z.S.; Wu, S.Q.; Kitagawa, Y.; Su, S.Q.; Huang, Y.G.; Li, G.L.; Ni, Z.H.; Nojiri, H.; Shiota, Y.; Yoshizawa, K.; et al. Anisotropic Change in the Magnetic Susceptibility of a Dynamic Single Crystal of a Cobalt(II) Complex. *Angew. Chem. Int. Ed.* **2017**, *56*, 717–721. [CrossRef]
72. Li, Y.; Wu, S.Q.; Xue, J.P.; Wang, X.L.; Sato, O.; Yao, Z.S.; Tao, J. A Molecular Crystal Shows Multiple Correlated Magnetic and Ferroelectric Switchings. *CCS Chem.* **2020**, *3*, 2464–2472. [CrossRef]
73. Venkataramani, S.; Jana, U.; Dommaschk, M.; Sönnichsen, F.D.; Tuczek, F.; Herges, R. Magnetic Bistability of Molecules in Homogeneous Solution at Room Temperature. *Science* **2011**, *331*, 445–448. [CrossRef]
74. Thies, S.; Sell, H.; Schütt, C.; Bornholdt, C.; Näther, C.; Tuczek, F.; Herges, R. Light-Induced Spin Change by Photodissociable External Ligands: A New Principle for Magnetic Switching of Molecules. *J. Am. Chem. Soc.* **2011**, *133*, 16243–16250. [CrossRef]
75. Su, S.Q.; Wu, S.Q.; Baker, M.L.; Bencok, P.; Azuma, N.; Miyazaki, Y.; Nakano, M.; Kang, S.; Shiota, Y.; Yoshizawa, K.; et al. Quenching and Restoration of Orbital Angular Momentum through a Dynamic Bond in a Cobalt(II) Complex. *J. Am. Chem. Soc.* **2020**, *142*, 11434–11441. [CrossRef] [PubMed]
76. Guionneau, P.; Le Gac, F.; Kaiba, A.; Costa, J.S.; Chasseau, D.; Létard, J.-F. A reversible metal–ligand bond break associated to a spin-crossover. *Chem. Commun.* **2007**, *36*, 3723–3725. [CrossRef] [PubMed]
77. Hay, M.A.; McMonagle, C.J.; Wilson, C.; Probert, M.R.; Murrie, M. Trigonal to Pentagonal Bipyramidal Coordination Switching in a Co(II) Single-Ion Magnet. *Inorg. Chem.* **2019**, *58*, 9691–9697. [CrossRef] [PubMed]

78. Du, S.N.; Su, D.; Ruan, Z.Y.; Zhou, Y.Q.; Deng, W.; Zhang, W.X.; Sun, Y.; Liu, J.L.; Tong, M.L. Reversible Switchability of Magnetic Anisotropy and Magnetodielectric Effect Induced by Intermolecular Motion. *Angew. Chem. Int. Ed.* **2022**, *61*, e202204700. [CrossRef] [PubMed]
79. Vogelsberg, C.S.; Garcia-Garibay, M.A. Crystalline molecular machines: Function, phase order, dimensionality, and composition. *Chem. Soc. Rev.* **2012**, *41*, 1892–1910. [CrossRef] [PubMed]
80. Li, W.; He, C.T.; Zeng, Y.; Ji, C.M.; Du, Z.Y.; Zhang, W.X.; Chen, X.M. Crystalline Supramolecular Gyroscope with a Water Molecule as an Ultrasmall Polar Rotator Modulated by Charge-Assisted Hydrogen Bonds. *J. Am. Chem. Soc.* **2017**, *139*, 8086–8089. [CrossRef] [PubMed]
81. Song, X.J.; Zhang, T.; Gu, Z.X.; Zhang, Z.X.; Fu, D.W.; Chen, X.G.; Zhang, H.Y.; Xiong, R.G. Record Enhancement of Curie Temperature in Host–Guest Inclusion Ferroelectrics. *J. Am. Chem. Soc.* **2021**, *143*, 5091–5098. [CrossRef] [PubMed]
82. Fu, D.W.; Zhang, W.; Cai, H.L.; Zhang, Y.; Ge, J.Z.; Xiong, R.G.; Huang, S.D. Supramolecular Bola-Like Ferroelectric: 4-Methoxyanilinium Tetrafluoroborate-18-crown-6. *J. Am. Chem. Soc.* **2011**, *133*, 12780–12786. [CrossRef] [PubMed]
83. Zhang, H.Y.; Lu, S.Q.; Chen, X.; Xiong, R.G.; Tang, Y.Y. The first high-temperature multiaxial ferroelectric host–guest inclusion compound. *Chem. Commun.* **2019**, *55*, 11571–11574. [CrossRef] [PubMed]
84. Siegler, M.A.; Hao, X.; Parkin, S.; Brock, C.P. $[Ni(H_2O)_6](NO_3)_2 \cdot$(15-crown-5)$\cdot 2H_2O$: Three phase transitions and an intermediate modulated phase stable over a range of ca 40 K. *Acta Cryst. B* **2011**, *67*, 486–498. [CrossRef] [PubMed]
85. Tong, Y.B.; Tian, Z.F.; Duan, H.B.; Zhu, Z.P.; He, W.; Hong, T.Y.; Yu, G.; He, Y.J.; Yang, J.K. [(18-Crown-6)K][Fe(1)$Cl(1)_4]_{0.5}$[Fe(2)$Cl(2)_4]_{0.5}$: A Multifunctional Molecular Switch of Dielectric, Conductivity and Magnetic Properties. *Chem. Asian J.* **2018**, *13*, 656–663. [CrossRef] [PubMed]
86. Tang, Y.Z.; Gu, Z.F.; Xiong, J.-B.; Gao, J.X.; Liu, Y.; Wang, B.; Tan, Y.H.; Xu, Q. Unusual Sequential Reversible Phase Transitions Containing Switchable Dielectric Behaviors in Cyclopentyl Ammonium 18-Crown-6 Perchlorate. *Chem. Mater.* **2016**, *28*, 4476–4482. [CrossRef]
87. Zhang, Y.F.; Di, F.F.; Li, P.F.; Xiong, R.G. Crown Ether Host-Guest Molecular Ferroelectrics. *Chem. Eur. J.* **2022**, *28*, e202102990. [CrossRef]
88. Rado, G.T.; Folen, V.J. Observation of the Magnetically Induced Magnetoelectric Effect and Evidence for Antiferromagnetic Domains. *Phys. Rev. Lett.* **1961**, *7*, 310–311. [CrossRef]
89. Kimura, T.; Goto, T.; Shintani, H.; Ishizaka, K.; Arima, T.; Tokura, Y. Magnetic control of ferroelectric polarization. *Nature* **2003**, *426*, 55–58. [CrossRef] [PubMed]
90. Hur, N.; Park, S.; Sharma, P.A.; Ahn, J.S.; Guha, S.; Cheong, S.W. Electric polarization reversal and memory in a multiferroic material induced by magnetic fields. *Nature* **2004**, *429*, 392–395. [CrossRef]
91. Dos santos-García, A.J.; Solana-Madruga, E.; Ritter, C.; Andrada-Chacón, A.; Sánchez-Benítez, J.; Mompean, F.J.; Garcia-Hernandez, M.; Sáez-Puche, R.; Schmidt, R. Large Magnetoelectric Coupling Near Room Temperature in Synthetic Melanostibite Mn_2FeSbO_6. *Angew. Chem. Int. Ed.* **2017**, *56*, 4438–4442. [CrossRef]
92. Wang, Y.X.; Ma, Y.; Chai, Y.; Shi, W.; Sun, Y.; Cheng, P. Observation of Magnetodielectric Effect in a Dysprosium-Based Single-Molecule Magnet. *J. Am. Chem. Soc.* **2018**, *140*, 7795–7798. [CrossRef]
93. Wang, Y.X.; Shi, W.; Li, H.; Song, Y.; Fang, L.; Lan, Y.; Powell, A.K.; Wernsdorfer, W.; Ungur, L.; Chibotaru, L.F.; et al. A single-molecule magnet assembly exhibiting a dielectric transition at 470 K. *Chem. Sci.* **2012**, *3*, 3366–3370. [CrossRef]
94. Huang, B.; Zhang, J.Y.; Huang, R.K.; Chen, M.K.; Xue, W.; Zhang, W.X.; Zeng, M.H.; Chen, X.M. Spin-reorientation-induced magnetodielectric coupling effects in two layered perovskite magnets. *Chem. Sci.* **2018**, *9*, 7413–7418. [CrossRef]
95. Tian, Y.; Shen, S.; Cong, J.; Yan, L.; Wang, S.; Sun, Y. Observation of Resonant Quantum Magnetoelectric Effect in a Multiferroic Metal–Organic Framework. *J. Am. Chem. Soc.* **2016**, *138*, 782–785. [CrossRef] [PubMed]
96. Kagawa, F.; Horiuchi, S.; Tokunaga, M.; Fujioka, J.; Tokura, Y. Ferroelectricity in a one-dimensional organic quantum magnet. *Nat. Phys.* **2010**, *6*, 169–172. [CrossRef]
97. Li, D.; Wang, X.; Zhao, H.X.; Ren, Y.P.; Zhuang, G.L.; Long, L.S.; Zheng, L.S. The Mechanism of the Magnetodielectric Response in a Molecule-Based Trinuclear Iron Cluster Material. *Angew. Chem. Int. Ed.* **2020**, *59*, 14409–14413. [CrossRef] [PubMed]
98. Akiyoshi, R.; Zenno, H.; Sekine, Y.; Nakaya, M.; Akita, M.; Kosumi, D.; Lindoy, L.F.; Hayami, S. A Ferroelectric Metallomesogen Exhibiting Field-Induced Slow Magnetic Relaxation. *Chem. Eur. J.* **2022**, *28*, e202103367. [CrossRef]
99. Harding, D.J.; Harding, P.; Phonsri, W. Spin crossover in iron(III) complexes. *Coord. Chem. Rev.* **2016**, *313*, 38–61. [CrossRef]
100. Kumar, K.S.; Heinrich, B.; Vela, S.; Moreno-Pineda, E.; Bailly, C.; Ruben, M. Bi-stable spin-crossover characteristics of a highly distorted $[Fe(1\text{-}BPP\text{-}COOC_2H_5)_2](ClO_4)_2 \cdot CH_3CN$ complex. *Dalton. Trans.* **2019**, *48*, 3825–3830. [CrossRef]
101. Halcrow, M.A. Spin-crossover Compounds with Wide Thermal Hysteresis. *Chem. Lett.* **2014**, *43*, 1178–1188. [CrossRef]
102. Grzywa, M.; Röß-Ohlenroth, R.; Muschielok, C.; Oberhofer, H.; Błachowski, A.; Żukrowski, J.; Vieweg, D.; von Nidda, H.-A.K.; Volkmer, D. Cooperative Large-Hysteresis Spin-Crossover Transition in the Iron(II) Triazolate $[Fe(ta)_2]$ Metal–Organic Framework. *Inorg. Chem.* **2020**, *59*, 10501–10511. [CrossRef]